Theoretical study of magneto-excitons in the [111] GaAs quantum well

1997 J. Phys.: Condens. Matter 9 6257

(http://iopscience.iop.org/0953-8984/9/29/011)

J. Phys.: Condens. Matter **9** (1997) 6257–6265. Printed in the UK PII: S0953-8984(97)81291-X

Theoretical study of magneto-excitons in the [111] GaAs quantum well

M H Zhang, Q Huang and J M Zhou

Institute of Physics, Chinese Academy of Sciences, Beijing 100080, People's Republic of China

Received 24 January 1997, in final form 18 March 1997

Abstract. A Landau-level basis is used to calculate the magneto-excitons in a 110 Å [111] GaAs quantum well. The excitation spectra of heavy-hole and light-hole excitons are calculated with and without the axial approximation. It is found that the anisotropy of the valence-band structure can cause coupling between optically active and inactive heavy-hole excitons obtained in the axial approximation, and make the latter become optically active. We suggest that the experimentally observed doubly resonant Raman scattering peaked at 13 T magnetic field should take place for (σ^-, σ^-) polarization, and that it is caused by the LO-phonon Fröhlich scattering with a nonzero in-plane wave vector of the phonon.

1. Introduction

During the last twenty years, people have studied excitons in semiconductor quantum wells extensively, by means of absorption, excitation, photoluminescence, Raman scattering, and other techniques [1–7]. Of special interest are the properties of excitons in external fields. A magnetic field can change the electronic structure of the excitons. Thus, magnetic luminescence, magnetic excitation spectra, and magnetic Raman scattering have been used to study the properties of excitons. Many interesting phenomena have been found and studied [8–15]. Previous studies show [8–14] that for magneto-Raman scattering involving LO phonons, the Fröhlich scattering mechanism acts with two heavy-hole or two light-hole magneto-exciton states as the intermediate states for $(\sigma^{\pm}, \sigma^{\pm})$ polarizations, while deformation potential scattering acts between one heavy-hole and one light-hole magneto-exciton state for intermediate states for $(\sigma^{\pm}, \sigma^{\mp})$ polarizations. In both mechanisms, the same Landau index of two intermediate states is also required for LO-phonon magneto-Raman scattering. When the energy difference of incoming and outgoing intermediate exciton states is just the energy of one LO phonon, a doubly resonant Raman scattering (DRRS) can take place. Recently, Calleja *et al* have measured the excitation spectra and DRRS in [100] and [111] GaAs multiple quantum wells under a magnetic field [13, 14]. In the [100] GaAs quantum well, they found that, in some cases, DRRS could take place between two light-hole magneto-exciton states for $(\sigma^{\pm}, \sigma^{\pm})$ polarizations but different Landau indices. They pointed out that a complete understanding of such DRRSs must consider an additional elastic scattering process (for example, interface roughness scattering); thus, LO phonons with nonzero in-plane wave vector can take part in Raman scattering [14]. This kind of Raman scattering is a fourth-order process. In a 100 Å [111] $GaAs/Al_{0.35}Ga_{0.65}As$ quantum well, their experiment showed that a DRRS took place for a 13 T magnetic field and (σ^-, σ^+) polarization between two light-hole magneto-exciton

0953-8984/97/296257+09$19.50

states with different Landau indices. This experimental result is very surprising. Different polarizations of incident and scattering light mean different spins of the light-hole excitons, and different spins of the electrons in two excitons. In general Raman scattering processes, the spin of the electron is not changed. In this study we have made calculations for magneto-excitons in a [111] quantum well with the above structure, and find that a DRRS only can take place at about 13 T magnetic field and for (σ^-, σ^-) polarization. Besides the involvement of one LO-phonon scattering process, it also needs the help of an additional elastic scattering process. Another goal of the present study is to show how the large anisotropy of the valence band in a [111] quantum well affects magneto-exciton transitions. For [100] GaAs quantum wells, Goldoni *et al* found that the anisotropy of the valence band could cause anticrossing behaviour for high magnetic fields [15]. [111] quantum wells, have lower symmetry than [100] quantum wells, and thus are expected to exhibit interesting phenomena.

We use the effective-mass theory proposed by Bauer and Ando to study magneto-excitons [16]. Instead of the eigenfunctions of a two-dimensional hydrogen atom, we use Landau levels as the basis for the radial wavefunction in the plane of the quantum well. Such a basis is appropriate at high magnetic field. It was previously believed that, for quantum wells, the convergence is very slow when one uses Landau levels as the basis for the radial wavefunction of the magneto-exciton, due to the strong Coulomb interaction. This is the case for the strictly two-dimensional magneto-exciton; in [17], 1500 Landau levels were used to obtain convergence. However, for real GaAs quantum wells, due to the finite width of the well and the finite height of the barrier, the exciton binding energy is about 10 meV, which is smaller than the value of 16.5 meV found for the strictly two-dimensional case. Our recent study [18] finds that just using more than ten Landau levels for each spin component of the magneto-exciton can give a good description for magneto-excitons in [100] GaAs quantum wells.

In this paper, we use Landau levels as the basis for the radial wavefunction of the exciton, in calculating the excitation spectra of magneto-excitons in a 110 Å [111] GaAs quantum well; such a well was investigated in Calleja's experiment. The paper is organized as follows. The theoretical framework is detailed in section 2. In section 3, the excitation spectra without and with the anisotropy, and the mechanism of the DRRS are discussed. Finally, conclusions are given in section 4.

2. The theoretical framework

Bauer and Ando studied excitons in [100], [110], and [111] quantum wells [16]. The explicit exciton Hamiltonian for the [111] quantum well is not given in their paper; we derive it by following the procedure that they outlined. In this paper, the atomic units $m_0 = \frac{1}{2}, \bar{h} = 1$, and $e^2 = 2$ are used. Energies, measured relative to the band gap of GaAs, will be expressed in rydbergs (R_0), lengths in Bohr radii (a_0), and magnetic fields in terms of the dimensionless quantity γ:

$$\gamma = \frac{e\bar{h}H}{2m_0cR_0} = \frac{1}{\ell^2} \tag{1}$$

where ℓ is the magnetic length, and the other symbols have their usual meaning.

In the effective-mass approximation, the μth eigenstate of an exciton with zero momentum of the centre of mass in the plane of the quantum well can be written as

$$\varphi^{\mu}_{ex}(\boldsymbol{r}_e, \boldsymbol{r}_h) = \sum_{M_e, M'} F^{\mu}_{M_e, M'}(\boldsymbol{\rho}, z_e, z_h)\varphi^{c}_{M_e}(\boldsymbol{r}_e)\hat{K}\varphi^{v}_{M'}(\boldsymbol{r}_h). \tag{2}$$

The arguments in equation (2) are the coordinates of the hole and the electron, $\boldsymbol{r}_h = (x_h, y_h, z_h)$ and $\boldsymbol{r}_e = (x_e, y_e, z_e)$, and the difference coordinates in the plane of the well, $\boldsymbol{\rho} = (x_h - x_e, y_h - y_e, 0)$. $\varphi^c_{M_e}$, $\varphi^v_{M'}$ denote the Bloch functions of conduction- and valence-band electrons, where M_e and M' are magnetic quantum numbers, i.e., $M_e = (\frac{1}{2}, -\frac{1}{2})$ for the conduction band, and $M' = (\frac{3}{2}, \frac{1}{2}, -\frac{1}{2}, -\frac{3}{2})$ for the valence band. $\hat{K}$ denotes the time-inversion operator, which transforms the Bloch function of the valence-band electron into that of a hole. $F^{\mu}_{M_e,M'}(\boldsymbol{\rho}, z_e, z_h)$ are the components of the μth-exciton envelope function, with arguments $\boldsymbol{\rho}$, z_e, and z_h; they diagonalize the effective-mass-type exciton Hamiltonian H_{ex}:

$$\sum_{L_e,L'} (H_{ex})_{M_eM',L_eL'} F^{\mu}_{L_eL'} = E^{\mu}_{ex} F^{\mu}_{M_eM'}. \tag{3}$$

If we neglect the electron–hole exchange interaction, then the eight-dimensional matrix equation (3) reduces to two four-dimensional equations for spin-up and spin-down conduction-band electrons.

The exciton envelope function is expanded as follows:

$$F^{\mu}_{M_eM'}(\boldsymbol{\rho}, z_e, z_h) = \sum_{n,m,i,j} C^{\mu M_eM'}_{nmij} \xi^{M_e}_i(z_e) \xi^{M'}_j(z_h) R_{nm}(\boldsymbol{\rho}). \tag{4}$$

$\{R_{nm}\}$ is a set of basis functions in the (ρ, ϕ) plane, with m as the magnetic quantum number. Here they are taken as Landau levels, and will be given in the following. The ξs denote the subband envelope functions of the quantum well for zero in-plane wave vector in the absence of a magnetic field; they are solutions of the one-dimensional effective-mass equation. The effective masses for the electron, heavy hole, and light hole are m^z_e, $m^{\pm 3/2}_h = 1/(\gamma_1 - 2\gamma_3)$, and $m^{\pm 1/2}_h = 1/(\gamma_1 + 2\gamma_3)$, respectively.

Following [19] and [20], we take the Landau levels as follows:

$$R_{n,m}(\boldsymbol{\rho}) \equiv \phi_{nn'}(\boldsymbol{\rho}) = \frac{(a^+)^n (b^+)^{n'}}{\sqrt{n!n'!}} \phi_{00}(\boldsymbol{\rho}) \qquad \text{with } m = n - n' \tag{5}$$

$$\phi_{00}(\boldsymbol{\rho}) = \frac{1}{\sqrt{2\pi}\ell} \exp\left(-\left(\frac{\rho}{2\ell}\right)^2\right). \tag{6}$$

Here a, a^+, b, and b^+ are the Bose operators defined in [19] and [20]. The value of the s-type wavefunction ϕ_{nn} at $\rho = 0$ is $(-1)^n/\sqrt{2\pi}\ell$.

Using these Landau levels as the basis functions for the radial functions of the excitons, we have the following exciton Hamiltonian for a [111] quantum well:

$$H_{ex} = \begin{pmatrix} A_{3/2} & B & C & 0 \\ B^* & A_{1/2} & 0 & C \\ C^* & 0 & A_{-1/2} & -B \\ 0 & C^* & -B^* & A_{-3/2} \end{pmatrix} + \left(-\frac{2}{\epsilon|\boldsymbol{r}_e - \boldsymbol{r}_h|} \pm \frac{g_e}{2}\gamma\right)\mathbf{I}_4 \tag{7}$$

where

$$A_{\pm 3/2} = -\frac{1}{m^z_e}\frac{\partial^2}{\partial z_e^2} + V_c(z_e) - (\gamma_1 - 2\gamma_3)\frac{\partial^2}{\partial z_h^2} + V_v(z_h) + \left(\frac{1}{m^{\parallel}_h} + \frac{1}{m^{\parallel}_e}\right)\omega_c\left(a^+a + \frac{1}{2}\right) - \frac{1}{m^{\parallel}_h}\omega_c L_z \pm \left(3\kappa + \frac{23}{4}q\right)\gamma \tag{8}$$

$$A_{\pm 1/2} = -\frac{1}{m^z_e}\frac{\partial^2}{\partial z_e^2} + V_c(z_e) - (\gamma_1 + 2\gamma_3)\frac{\partial^2}{\partial z_h^2} + V_v(z_h)$$

$$+\left(\frac{1}{m_l^{\parallel}}+\frac{1}{m_e^{\parallel}}\right)\omega_c\left(a^+a+\frac{1}{2}\right)-\frac{1}{m_l^{\parallel}}\omega_c L_z\pm\left(\kappa+\frac{13}{4}q\right)\gamma \tag{9}$$

$$B=2\sqrt{3\omega_c}\bar{\gamma}_2 b\frac{\partial}{\partial z_h}-\frac{2\sqrt{6}}{3}\omega_c u(b^+)^2 \tag{10}$$

$$C=\sqrt{3}\omega_c\bar{\gamma}_1 b^2+\frac{2\sqrt{6\omega_c}}{3}ub^+\frac{\partial}{\partial z_h} \tag{11}$$

$$m_h^{\parallel}=\frac{1}{\gamma_1+\gamma_3}\qquad m_l^{\parallel}=\frac{1}{\gamma_1-\gamma_3} \tag{12}$$

$$\bar{\gamma}_1=\frac{2\gamma_2+\gamma_3}{3}\qquad \bar{\gamma}_2=\frac{\gamma_2+2\gamma_3}{3} \tag{13}$$

$$u=(\gamma_2-\gamma_3). \tag{14}$$

Here ω_c is the cyclotron frequency of a free electron: $\omega_c=2/\ell^2$. $L_z=a^+a-b^+b$ is the angular momentum operator in this representation. $\gamma_1,\gamma_2,\gamma_3$, κ, and q are the Luttinger valence-band parameters. g_e is the g-factor of the conduction-band electron. We distinguish the in-plane electron effective mass $m_e^{\parallel}$ from the z-direction electron effective mass m_e^z, to account for the effects of nonparabolicity of the conduction band [15]. In the following, we take $m_e^{\parallel}$ as a parameter, to fit to the experimental fan plot of magneto-exciton transitions. $\mathbf{I}_4$ denotes the 4×4 unit matrix.

In order to include the excitonic effects, we should calculate Coulomb matrix elements. The mathematical details are presented in the appendix.

The oscillator strength has been given by Bauer and Ando [16]. For the μth exciton, it is

$$f_{ex}^{\mu}=f_{M_eM'_\mu}^{B}\frac{E_g}{E_{ex}^{\mu}+E_g}\left|\sum_{n,i,j}C_{n0ij}^{\mu M_eM'_\mu}R_{n0}(0)\int \mathrm{d}z\ \xi_i^{M_e}(z)\xi_j^{M'_\mu}(z)\right|^2. \tag{15}$$

Here $f_{M_eM'_\mu}^{B}$ is the oscillator strength of a band-to-band transition in the bulk crystal; the value for the heavy hole is three times as large as the one for the light hole.

Finally, we discuss the expansion of the radial functions of the excitons. If we make use of the axial approximation, e.g. setting $u=0$ in equations (10) and (11), then the total angular momentum of the exciton in the z-direction is a good quantum number. The magnetic quantum numbers of the radial functions $\{R_{nm}\}$ for the four spin components are $(i+3;i+2;i+1;i)$ with i as an integer. According to the selection rules [16], under σ^- incoming light, only the σ^- exciton fulfilling the condition $M_e-M'_\mu=-1$ can be excited, with M_e as the spin of the electron and M'_μ as the spin component of the hole, which has s-type radial wavefunctions; similarly, under σ^+ incoming light, only the σ^+ exciton fulfilling the condition $M_e-M'_\mu=1$ can be excited. $M_p\equiv M_e-M'_\mu$ is defined as the spin of the exciton in [21]. For optically active excitons, i takes following values: $i=0$ and $i=-3$ for the σ^+ and σ^- heavy-hole excitons, respectively; and $i=-1$ and $i=-2$ for the σ^+ and σ^- light-hole excitons, respectively. Adding the anisotropy of the valence band, the magnetic quantum number of the radial functions $\{R_{nm}\}$ for each component does not have a definite value; we take 3 as the maximum of the absolute values of the magnetic quantum numbers, and obtain the following expansions for heavy- and light-hole excitons.

In table 1, columns (a) are for the σ^+ light-hole exciton with $M_e=-\frac{1}{2}$, columns (b) are for the σ^- light-hole exciton with $M_e=\frac{1}{2}$, and columns (c) correspond to the σ^- heavy-hole exciton in the case where $M_e=\frac{1}{2}$, and to the σ^+ heavy-hole exciton in the case where $M_e=-\frac{1}{2}$. In the axial approximation, if $M_e=\frac{1}{2}$, we can obtain two kinds of

Table 1. Magnetic quantum numbers in the expansion of the radial functions $\{R_{nm}\}$ including the anisotropy of the valence band. The two sets of columns (a) and (b) are for σ^- and σ^+ light-hole excitons, respectively. Columns (c) are for both σ^- and σ^+ heavy-hole excitons.

	(a)			(b)			(c)		
3/2	−2	1		−1	2		−3	0	3
1/2	−3	0	3	−2	1			−1	2
−1/2		−1	2	−3	0	3		−2	1
−3/2		−2	1		−1	2	−3	0	3

heavy-hole exciton state denoted by (0, −1, −2, −3) and (3, 2, 1, 0); the former has spin $M_p = -1$ and is optically active, while the latter has spin $M_p = 2$ and is optically inactive. These two kinds of state are coupled together by the anisotropy according to columns (c) in table 1, making the latter become optically active. For $M_e = -\frac{1}{2}$, we obtain similar results.

3. Computational results

Using the above method, we have calculated the excitation spectra of magneto-excitons for a [111] $GaAs/Al_{0.35}Ga_{0.65}As$ quantum well; such a well was investigated in Calleja's experiment [13]. The nominal width of the well is 100 Å. We find that the calculated results obtained using 110 Å as the width are in better agreement with the experimental ones. For simplicity, we use effective-mass parameters of GaAs for both the well and the barrier. The fundamental gap of $Al_xGa_{1-x}As$ is taken as $1.519 + 1.155x + 0.37x^2$ eV. The 70:30 rule is chosen for the ratio of the conduction-band offset to the valence-band one. All of the parameters used are given in table 2. The zero point of the energy in the following is chosen to lie at the position of the fundamental gap of GaAs. For the basis functions in the z-direction, we have used all bound states: six subbands for heavy holes and two for light holes. The number of Landau levels is 15 for each angular momentum component of the radial wavefunction in practical calculations. We find that $m_e^{\parallel} = 0.073$ can give good agreement with experimental results.

Table 2. Effective-mass parameters of GaAs.

m_e^z	0.067
$m_e^{\parallel}$	0.073
γ_1	6.85
γ_2	2.1
γ_3	2.9
E_g	1.519 eV
κ	1.2
q	0.04
g_e	−0.44
ϵ	12.5

In figures 1(a) and 1(b) we present excitation spectra of σ^- and σ^+ heavy-hole excitons. For each magnetic field, two curves are given: the upper one is calculated in the axial approximation, while the lower one is obtained with the anisotropy included. Strong

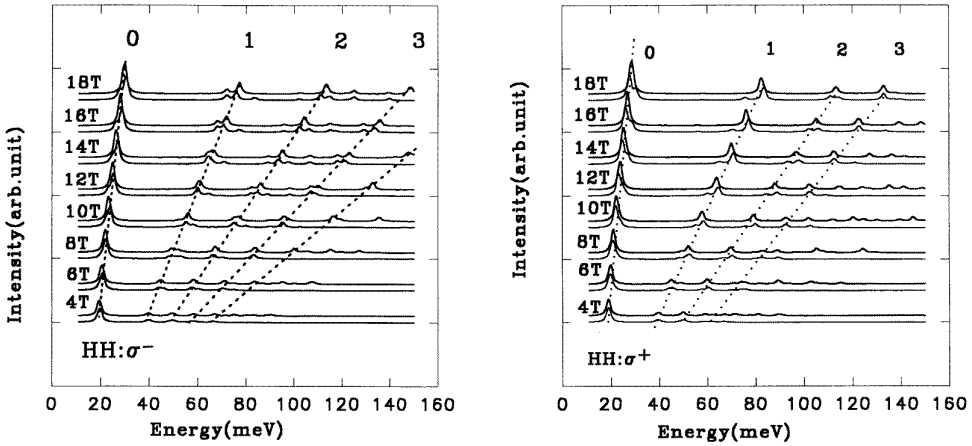

(a) (b)

Figure 1. Excitation spectra of heavy-hole excitons: (a) σ^- polarization and (b) σ^+ polarization. For each magnetic field, the upper curve is calculated in the axial approximation, while the lower is calculated by including the anisotropy.

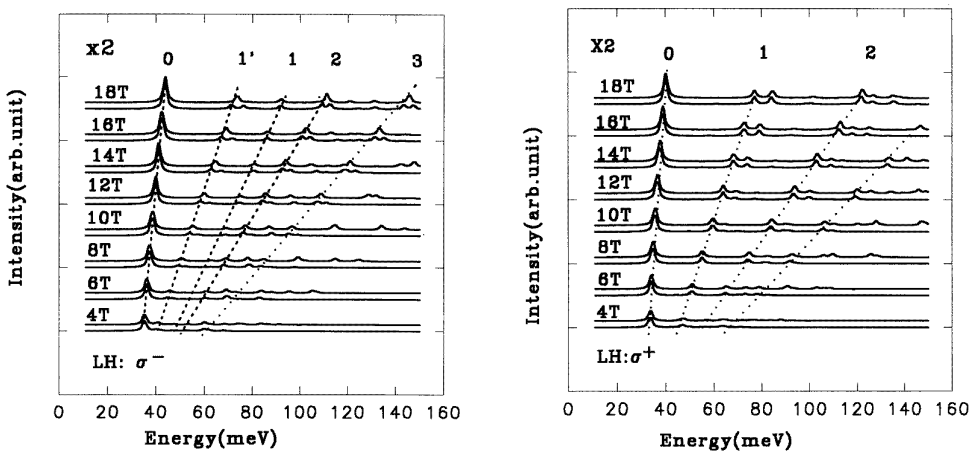

(a) (b)

Figure 2. Excitation spectra of light-hole excitons: (a) σ^- polarization and (b) σ^+ polarization. For each magnetic field, the upper curve is calculated in the axial approximation, while the lower is calculated by including the anisotropy.

transitions are labelled according to the dominant Landau level. The anisotropy makes the original dark heavy-hole excitons become optically active; thus, each original transition is split into two components; one is weaker, and the other is stronger. In figure 1(a), the energy difference between the weaker and stronger components in the lowest heavy exciton, labelled as 0, is about 1 meV in a field of 4 T, and increases to 2.5 meV in a field of 16 T. The ratio of the oscillator strength for the weaker one to that for the stronger one is 0.18 in a field of 4 T and 0.31 in a field of 16 T. Similar behaviour can be found in figure 1(b) for transitions of σ^+ heavy-hole excitons. We note that the transitions labelled as 0, 1, and

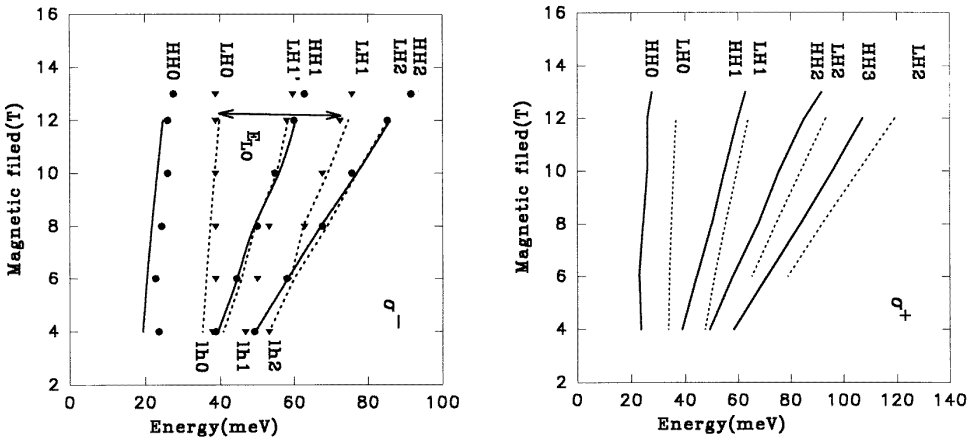

(a) (b)

Figure 3. A comparison of the calculated fan plots of exciton transitions and the experimental ones: (a) under σ^--polarized incoming light and (b) under σ^+-polarized incoming light. Solid lines represent calculated heavy-hole exciton transitions, while dotted lines represent calculated light-hole exciton transitions. The experimental spectra are represented by solid circles for heavy-hole exciton transitions, and by solid triangles for light-hole exciton transitions, and were taken from [13].

2 have opposite energy orders for the weaker and stronger components in figure 1(a) and figure 1(b). The coupling between excitons with different spins should manifest its role in the spin dynamics of the exciton. We suggest that experimental study of this problem would be very interesting. Maialle *et al* have studied the spin dynamics of the exciton in [100] GaAs quantum wells, where the effect of the anisotropy of the valence band on the ground state of the heavy-hole exciton is small and is neglected [21]. In figures 2(a) and 2(b), we present the calculated excitation spectra for light-hole excitons. The results show that the anisotropy has less influence on light-hole excitons. In figure 2(a), the transitions labelled $1'$ and 1 both acquire nonzero oscillator strength through the Landau level $\phi_{1,1}$ in the spin component $M' = \frac{1}{2}$; however, the latter one has a smaller oscillator strength than the former. Coulomb interaction has large effects on the transition $1'$, which receives its dominant (52%) contribution from the Landau level $\phi_{0,2}$ in the first heavy-hole subband and the spin component $M' = -\frac{3}{2}$. In figure 2(b), corresponding to transitions $1'$ and 1 in figure 2(a), there are also two transitions in high magnetic fields; however, they have a smaller energy difference than that between transitions $1'$ and 1 in figure 2(a), so we denote both of them as transition 1. The anisotropy of the valence band causes transitions $1'$, 2, and 3 to split into doublets in figure 2(a), while it has almost no influence on the energies of the σ^+ light-hole excitons. It should be mentioned that the scale of the intensity in the excitation spectra of the light-hole exciton is enlarged by a factor of 2 compared to that of the heavy-hole exciton. In figure 3(a), we have compared a calculated fan plot of the strong exciton transitions with the experimental one. For heavy-hole exciton transitions, the agreement is very good. The experimental light-hole exciton transitions are labelled lh0, lh1, and lh2 using notation from Calleja *et al* [13]. Our calculated transitions LH0 and LH1 are in agreement with lh0 and lh2, respectively, while our calculated transitions $LH1'$ and LH2 coincide with HH1 and HH2, respectively. No calculated transition corresponds to the experimentally observed transition lh1. We note that the transition HH1 in figure 1(a) is

composed of several transitions. We think that it is very difficult to separate the light-hole exciton transition from the heavy hole one experimentally near the transition HH1. The very weak intensity of lh1 in [13] makes us believe that our results are reliable. As a comparison, the fan plot of calculated σ^+ exciton transitions is presented in figure 3(b).

Next we discuss the mechanism of experimentally observed DRRS peaked for 13 T magnetic field and (σ^-, σ^+) polarization. The reported DRRS takes place between lh2(σ^-) as the incoming intermediate exciton state and lh0(σ^+) as the outgoing intermediate exciton state. The possibility of such a DRRS is very small, because, in general Raman scattering processes, the spin of the electron is not changed. There might be a misprint in [13]. Our calculation finds that at 12.5 T the energy difference between LH1(σ^-) and LH0(σ^-) is just the energy of one LO phonon (36.5 meV) meeting the energy condition for the DRRS. Although a LO phonon with zero in-plane wave vector cannot be emitted between the above two states in a one-phonon Raman process, due to the orthogonality of their radial wavefunctions, a fourth-order process such as a DRRS can take place by means of Fröhlich scattering. The fourth-order process has been observed in the [100] GaAs quantum well [14], where interface roughness scattering involving resonant Raman scattering has been proposed to explain the anomalous DRRS. An additional elastic scattering mechanism can cause the LO phonon with nonzero in-plane wave vector to take part in the Raman scattering process. The DRRS discussed here is, we think, caused by a similar mechanism.

4. Conclusions

In summary, we have made calculations for magneto-excitons in 110 Å [111] GaAs quantum wells. We find that the anisotropy of the valence-band structure can cause coupling between optically active and inactive heavy-hole excitons obtained in the axial approximation, and make the latter become optically active. We suggest that the experimentally observed doubly resonant Raman scattering peaked at 13 T magnetic field should take place for (σ^-, σ^-) polarization, and that it is caused by the LO-phonon Fröhlich scattering with a nonzero in-plane wave vector of the phonon.

Appendix

In order to include excitonic effects, we should calculate the following Coulomb matrix elements:

$$\int \mathrm{d}z_e \; \mathrm{d}z_h \int \mathrm{d}\boldsymbol{\rho} \; \xi_i^c(z_e)^* \xi_j^v(z_h)^* R_{n,m}(\boldsymbol{\rho})^* \frac{1}{|\boldsymbol{r}_e - \boldsymbol{r}_h|} \xi_{i'}^c(z_e) \xi_{j'}^v(z_h) R_{n',m'}(\boldsymbol{\rho}). \tag{A1}$$

We can separate the integration in the plane of the well from the one normal to the well by expressing the Coulomb interaction in terms of the following Fourier integral:

$$\frac{1}{|\boldsymbol{r}_e - \boldsymbol{r}_h|} = \int \frac{\mathrm{d}\boldsymbol{q}}{2\pi} \; \frac{\mathrm{e}^{-q|z_e - z_h|}}{q} \mathrm{e}^{\mathrm{i}\boldsymbol{q}\cdot\boldsymbol{\rho}}. \tag{A2}$$

It is very easy to see that the only nonzero matrix element connects two radial functions with the same angular momentum. The radial integrals are of the type

$$\int \mathrm{d}\boldsymbol{\rho} \; R_{n,m}(\boldsymbol{\rho})^* R_{n',m'}(\boldsymbol{\rho}) \mathrm{e}^{\mathrm{i}\boldsymbol{q}\cdot\boldsymbol{\rho}}. \tag{A3}$$

In the Landau-level basis, they can be calculated using a formula given in [22]. The z-direction integrals—form factors—are

$$\int \mathrm{d}z_e \int \mathrm{d}z_h \ \xi_i^c(z_e)^* \xi_j^v(z_h)^* \xi_{i'}^c(z_e) \xi_{j'}^v(z_h) \mathrm{e}^{-q|z_e - z_h|}. \tag{A4}$$

They can be transformed into the following integrals in the region of $z_e \in [d_{e1}, d_{e2}]$ and $z_h \in [d_{h1}, d_{h2}]$.

$$\int_{d_{e1}}^{d_{e2}} \mathrm{d}z_e \int_{d_{h1}}^{d_{h2}} \mathrm{d}z_h \ (\mathrm{e}^{\lambda_{e1} z_e} \mathrm{e}^{\lambda_{h1} z_h})^* (\mathrm{e}^{\lambda_{e2} z_e} \mathrm{e}^{\lambda_{h2} z_h}) \mathrm{e}^{-q|z_e - z_h|}. \tag{A5}$$

and can also be calculated analytically [16].

The remaining one-dimensional integrals involving the Fourier components q can be computed numerically by the Gauss quadrature method.

References

[1] Dingle R 1975 *Festörperprobleme (Advances in Solid State Physics)* vol 15, ed H J Queisser (Braunschweig: Vieweg)
[2] Miller R C, Kleinman D A, Tsang W T and Gossard A C 1981 *Phys. Rev.* B **22** 1134
[3] Miller R C, Gossard A C, Sanders G D, Chang Y C and Schulman J N 1985 *Phys. Rev.* B **32** 8452
[4] Maan J C, Belle G, Fasolino A, Altarelli M and Ploog K 1984 *Phys. Rev.* B **30** 2253
[5] Miller D A B, Chemla D S, Damen T C, Gossard A C, Wiegmann W, Wood T H and Burrus C A 1985 *Phys. Rev.* B **32** 1043
[6] Viña L, Collins R T, Mendez E E and Wang W I 1986 *Phys. Rev.* B **33** 5939
[7] Collins R T, Viña L, Wang W I, Chang L L, Esaki L, von Klitzing K and Ploog K 1987 *Phys. Rev.* B **36** 1531
[8] Ruf T, Philips R T, Trallero-Giner C and Cardona M 1990 *Phys. Rev.* B **41** 3039
[9] Trallero-Giner C, Ruf T and Cardona M 1990 *Phys. Rev.* B **41** 3028
[10] Cros A, Cantareo A, Trallero-Giner C and Cardona M 1992 *Phys. Rev.* B **45** 6106
[11] Cros A, Ruf T, Spitzer J, Cardona M and Cantareo A 1994 *Phys. Rev.* B **50** 2325
[12] Calle F, Calleja J M, Meseguer F, Viña L, López C and Ploog K 1991 *Phys. Rev.* B **44** 1113
[13] Calleja J M, Viña L, Berendschot T, Calle F, López C, Meseguer F, Tejedor C and Perenboom J A A J 1993 *Phonons in Semiconductor Nanostructures (NATO Advanced Study Institute, Series E, vol 236)* ed J P Leburton, J Pascual and C R Sotomayor-Torres (Dordrecht: Kluwer) p 121
[14] Viña L, Calleja J M, Cors A, Cantarero A, Berendschot T, Perenboom J A A J and Ploog K 1996 *Phys. Rev.* B **53** 3975
[15] Goldoni G, Ruf T, Sapega V F, Fainstein A and Cardona M 1995 *Phys. Rev.* B **51** 14 542
[16] Bauer G E W and Ando T 1988 *Phys. Rev.* B **38** 6015
[17] Stafford C, Schmitt-Rink S and Schäfer W 1990 *Phys. Rev.* B **41** 10 000
[18] Zhang M H, Huang Q and Zhou J M 1997 *Phys. Rev.* B submitted
[19] McDonald A H and Ritchie D S 1986 *Phys. Rev.* B **33** 8336
[20] Malkin I A and Man'ko V I 1969 *Sov. Phys.–JETP* **28** 527
[21] Maialle M Z, de Andrada e Silva E A and Sham L J 1993 *Phys. Rev.* B **47** 15 776
[22] Haug H and Koch S W 1994 *Quantum Theory of the Optical and Electronic Properties of Semiconductors* 3rd edn (Singapore: World Scientific)